

Determination of an onset of superconducting diamagnetism by scaling of the normal-state magnetization

I. L. Landau, K. M. Mogare, B. Trusch, M. Wagner, J. Hulliger

Department of Chemistry and Biochemistry, University of Berne, Freiestrasse 3, CH-3012-Berne, Switzerland

Abstract

We propose a simple scaling procedure for the normal-state magnetization M_n data collected as functions of temperature T in different magnetic fields H . As a result, the $M_n(T)$ curves collected in different fields collapse on to a single $M_{sc}(T)$ line. In this representation, the onset of superconducting diamagnetism manifests itself by a sharp divergence of the $M_{sc}(T)$ curves for different H values. As will be demonstrated, this allows for a reliable determination of temperature T_{onset} , at which superconducting diamagnetism become observable.

Key words: type-II superconductors, superconducting diamagnetism, normal-state magnetization, superconducting critical temperature

PACS: 74.60.-w, 74.-72.-h

1. Introduction

An onset of superconducting diamagnetism in a vicinity of the superconducting critical temperature T_c attracts a lot of attention in high- T_c superconductors [1–9]. This attention is partly dictated by an obvious fundamental interest to the onset of superconductivity in such complex materials. It is also important from purely practical reasons because it provides the highest value of T_c in non-uniform superconducting samples.

At the same time, in spite of apparent simplicity of the problem, experimental studies are rather complex. Because all high- T_c superconductors have a considerable temperature dependence of the normal-state magnetization M_n , extrapolation of M_n to a region of the superconducting transition is not obvious and sometimes question-

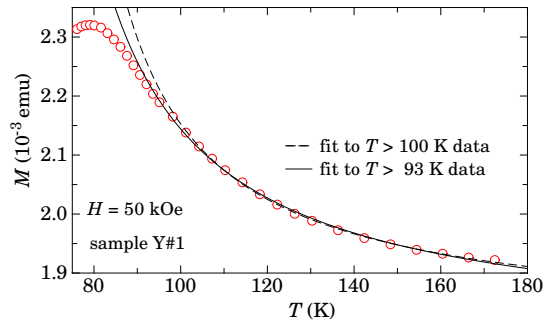


Fig. 1. Magnetization $M(T)$ data for Y#1 sample collected in a magnetic field $H = 50$ kOe. The solid and the dashed lines are fits of Eq. (1) for two sets of experimental data points.

able (see, for instance, Fig 1 of Ref. [8] and Figs. 8 and 9 in Ref. [9]).

As an example, Fig. 1 shows magnetization data

for an oxygen depleted sample of $\text{YBa}_2\text{Cu}_3\text{O}_{7-x}$. Detailed data for this sample will be presented and discussed below. We have tried to fit experimental $M_n(T)$ data by the Curie-Weisse law plus some temperature independent constant M_0 :

$$\chi = C/(T - \Theta) + M_0. \quad (1)$$

C , Θ and M_0 were used as fit parameters. As may be seen in Fig. 1, the calculated curves do not fit experimental data points particularly well. Furthermore, the corresponding values of the onset temperature T_{onset} noticeably depend on the data, which were chosen for approximation. In such and similar situations any conclusion about the onset of superconductivity is not reliable.

Here, we shall introduce a simple procedure to scale the normal-state magnetization data collected in different magnetic fields. Because the proposed procedure does not involve any specific assumption about sample properties, it is applicable to uniform and non-uniform samples, to single crystals and ceramics.

2. Samples

In this section we present a brief description of samples, which were used to verify the proposed scaling procedures. Two kinds of high- T_c materials were investigated: $\text{YBa}_2\text{Cu}_3\text{O}_{7-x}$ (YBCO) and $\text{Tl}_2\text{Ba}_2\text{Ca}_2\text{Cu}_3\text{O}_{10}$ (Tl-2223). All samples were ceramics and were not particularly uniform. Fig. 2 shows a superconducting transition for an oxygen depleted sample Y#1. The mean-field superconducting temperature T_c is defined as is shown in Fig. 2(a). Because this sample was kept on air for about a year, it contained inclusions with a higher level of doping and with correspondingly higher T_c values. This resulted in about 25 K long tale of the transition (see Fig. 2(b)). Definitions of the mean-field critical temperature T_c and $T_c^{(max)}$ are shown in Fig.2. Main characteristics of samples are summarized in Table 1.

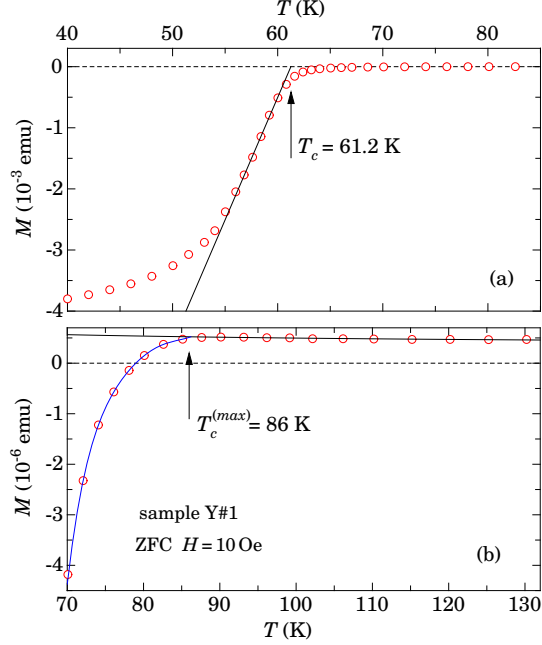


Fig. 2. Magnetization $M(T)$ data for Y#1 sample collected in a low magnetic field $H = 10$ Oe after zero-field-cooling (ZFC). (a) The main part of the transition. The solid line is a linear fit to the steepest part of the $M(T)$ curve. (b) A tale of the transition with y -scale expanded by three orders of magnitude. The solid line is a linear fit to $M(T)$ data at $T > 90$ K. Definitions of T_c and $T_c^{(max)}$ are shown in Figs. 2(a) and 2(b), respectively.

Table 1

Main parameters of samples. The effective magnetic field h_{f-p} characterizes a relative strength of a ferromagnetic contribution to the sample magnetization (see Eq. (4) for the definition)

sample	compound	T_c	T_c^{max}	h_{f-p}	T_{onset} (K)
Y#1	YBCO	61.2 K	86 K	0.14 kOe	88.5 ± 0.5
underdoped					
Y#2	YBCO	91.1 K	92 K	0.9 kOe	92.3 ± 0.2
Y#3	YBCO	91.2 K	92 K	1 kOe	92.5 ± 0.3
Tl#1	Tl-2223	122 K	130 K	0	131 ± 0.3
Tl#2	Tl-2223	100 K	125 K	2.9 kOe	125 ± 1

3. Scaling procedure

We consider two modifications of the scaling procedure. A simpler version is applicable to samples with purely paramagnetic normal-state magneti-

zation. If the normal-state magnetization includes also a ferromagnetic contribution, the procedure should be modified in order to account for a non-linearity of $M(H)$ curves.

3.1. Purely paramagnetic case

Because paramagnets may be described by a magnetic field independent magnetic susceptibility χ_p , the sample magnetization $M = \chi_p H$, i.e., M is proportional to H at any temperature. This means that $M_n(T)$ curves collected in different fields will collapse onto a single $M_{sc}(T)$ curve if

$$M_{sc}(H) = \frac{M(H, T)}{M(H, T_0)}, \quad (2)$$

where T_0 is any temperature well above T_c .

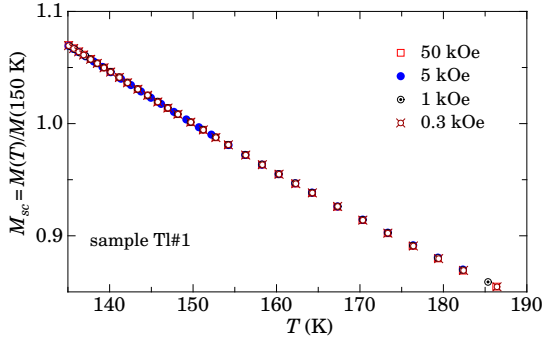


Fig. 3. Magnetization data for Tl#1 sample collected in four different fields plotted as $M_{sc} = M(T)/M(150 \text{ K})$ versus T

Fig. 3 illustrates results of such a scaling. Agreement between the data is practically perfect. While magnetic fields differ by more than two orders of magnitude, the differences between the $M_{sc}(T)$ curves do not exceed an experimental scatter.

The scaled magnetization curves for lower temperatures are shown in Fig. 4. It may be seen that the onset temperature $T_{onset} \approx 131 \text{ K}$. There is some experimental uncertainty, but there are no systematic errors, which may distort the conclusions.

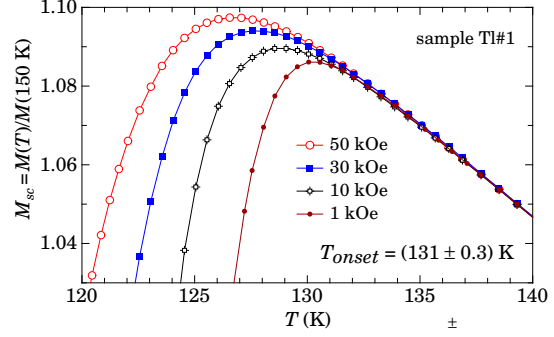


Fig. 4. The scaled magnetization data for the Tl#1 sample in the transition region. The solid lines are guides to the eye.

3.2. Paramagnetism with a ferromagnetic contribution

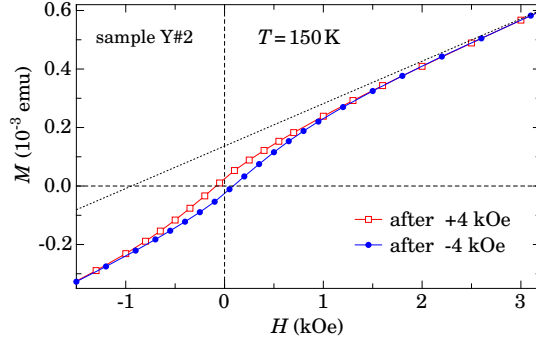


Fig. 5. Magnetization data for the sample Y#2 measured at $T = 150 \text{ K}$ in fields $-4 \text{ kOe} < H < 4 \text{ kOe}$. The solid lines are guides to the eye. The dotted line is a linear fit to data collected in fields $5 \text{ kOe} < H < 50 \text{ kOe}$.

Quite often, the normal-state magnetization of high- T_c superconductors cannot be described as purely paramagnetic. A typical example is shown in Fig. 5. There is a quite symmetrical hysteresis loop with non-zero magnetizations at $H = 0$, which is an unambiguous signature of ferromagnetism.

A simple scaling procedure, which was introduced in the previous subsection does not work, as may clearly be seen in Fig. 6. Because, the sample magnetization $M(H) = \chi H$ cannot be described with χ independent of field, this failure is expected.

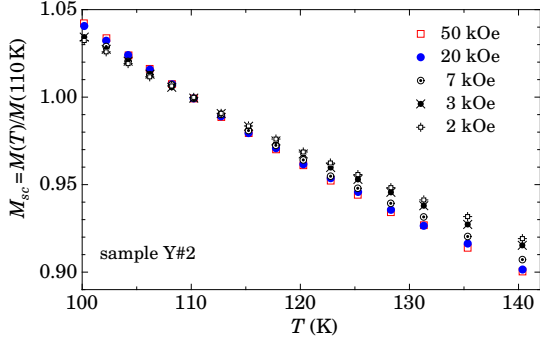


Fig. 6. $M(T)/M(110 \text{ K})$ measured in different fields as functions of temperature.

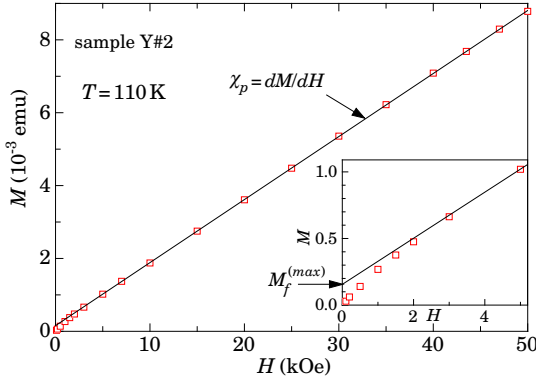


Fig. 7. M at $T = 110 \text{ K}$ versus field. The solid line is a linear fit to the data for $H \geq 5 \text{ kOe}$. The inset shows the low-field part of the curve on expanded scales. Arrows illustrate definitions of χ_p and $M_f^{(max)}$.

If there are several contributions to the sample magnetization, M may be written as a sum. In our case,

$$M = \chi_p H + M_f, \quad (3)$$

where indexes p and f are related to paramagnetic and ferromagnetic contributions, respectively. Fig. 7 shows $M(H)$ data for the same sample Y#2 measured in more details. As may be seen, for $H \geq 5 \text{ kOe}$, M is a linear function of H . This allows to conclude that all ferromagnetic inclusions are already saturated and in $H \geq 5 \text{ kOe}$ M_f is equal to its maximum value $M_f^{(max)}$. All calculations for this sample that we present below were made for $T_0 = 110 \text{ K}$. $\chi_p(T_0) = dM/dH \approx 1.73 \cdot 10^{-4}$

emu/kOe and $M_f^{(max)}(T_0) \approx 1.56 \cdot 10^{-4}$. In lower fields, M_f depends not just on field, but also on the magnetic history (see Fig. 4). However, $M_f(H)$ can easily be calculated by employing of Eq. (3).

In order to characterize a relative strength of a ferromagnetic contribution, we introduce

$$h_{f-p} = \frac{M_f^{(max)}}{\chi_p}. \quad (4)$$

The value of this effective field is a convenient way to characterize ferromagnetic contributions to M . The values of h_{f-p} for the investigated samples are presented in Table 1.

As the next step, we assume that $M_f(H)$ is temperature independent for all H values. This is the only realistic way to scale the normal-state magnetization data without making rather specific assumptions about sample properties, which may distort the final result. Although this cannot be exact, we shall show that in some limited temperature range above T_c this assumption works sufficiently well to ensure satisfactory scaling of experimental data. Thus, using Eq (3) and the value of $\chi_p(T_0)$, we calculate $M_f(H, T_0) = M - \chi_p H$. Then, experimental $M(T)$ data for different fields are scaled according to

$$M_{sc}(T) = \frac{M(H, T) - M_f(H, T_0)}{\chi_p(T_0)H} \quad (5)$$

The results of such scaling with $T_0 = 110 \text{ K}$ are presented in Fig. 8(a). As may be seen, $M_{sc}(T)$ curves calculated from experimental $M(T)$ data measured in different fields perfectly match each other in a rather extended temperature range $T > T_c$. The onset of diamagnetism is shown in Fig. 7(b). It can easily be established that $92 \text{ K} < T_{onset} < 92.7 \text{ K}$.

Similar results for the oxygen deficient sample Y#1 are shown in Fig. 9. As may be seen, $T_{onset} = (88.5 \pm 0.5) \text{ K}$. For this sample, $h_{f-p} = 0.14 \text{ kOe}$, i.e., a relative ferromagnetic contribution is approximately 6 times smaller than that for the sample Y#1.

Generally, a small ferromagnetic contribution favors good quality of scaling. However, the most important factor is not a low value of h_{f-p} , but rather temperature independence of $M_f(H)$, which is the

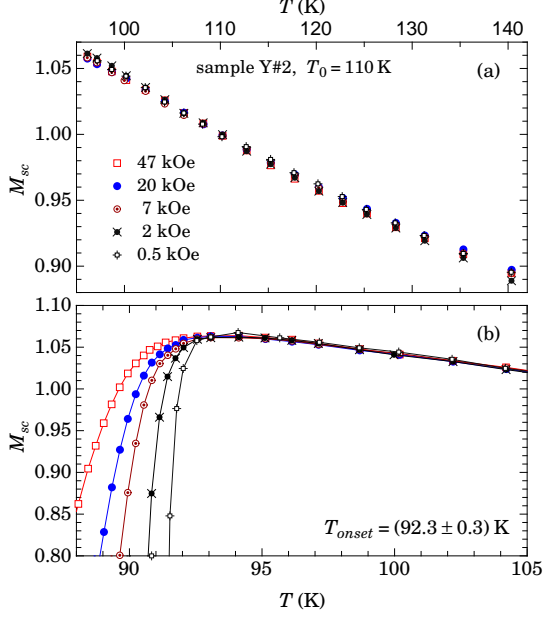


Fig. 8. Magnetization data for the sample Y#2 scaled according to Eq. (5) versus temperature. (a) For $T > T_c$. (b) In the transition region. The solid lines are guides to the eye.

basis of our scaling approach. For instance, for the sample Tl#2, $h_{f-p} = 3$ kOe, i.e., considerably higher than for all other samples presented here. Nevertheless, as may be seen in Fig. 10, $M_{sc}(T)$ curves calculated from data measured in different fields perfectly match each other in a rather extended ranges of temperatures and fields.

There were, however, some cases, in which the quality of scaling was not as good as presented above. The results for such a sample are shown in Fig. 11. While formal characteristics of this sample, including the value of h_{f-p} are quite similar to that of the sample Y#2 (see Table 1), quality of scaling for the sample Y#3 is not the same good (compare Figs. 8(a) and 11(a)). In the case of the sample Y#3, the data for $H \leq 5$ kOe deviate downwards from the master curve at higher temperatures (see Fig. 11(a)). Similar deviations upwards are visible at lower temperatures (see Fig. 11(b)).

The obvious reason is a noticeable dependence of $M_f(H)$ on temperature. We remind that the temperature independence of $M_f(H)$ is the basis of

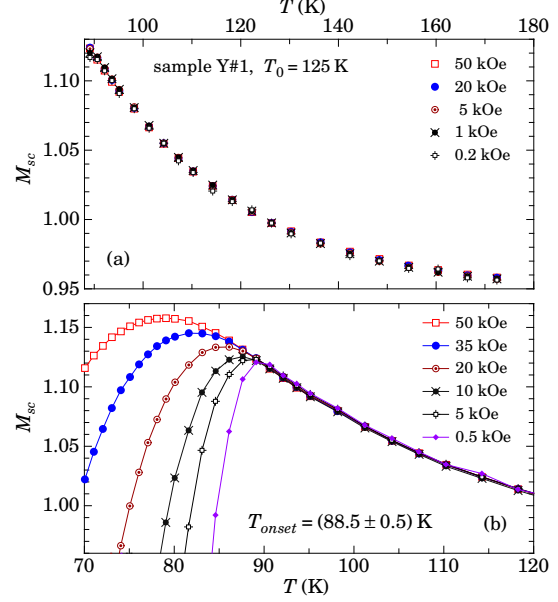


Fig. 9. M_{sc} for the sample Y#1 versus temperature. (a) For $T > T_c$. (b) In the transition region. The solid lines are guides to the eye

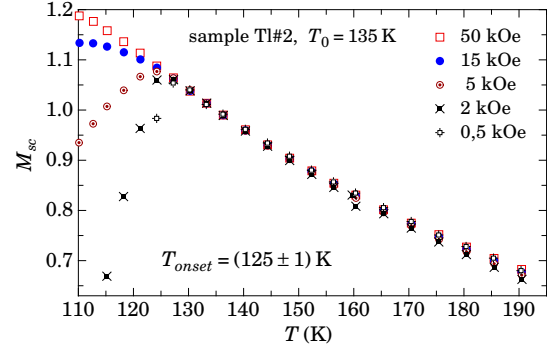


Fig. 10. M_{sc} versus T for the sample Tl#2.

this scaling procedure. At the same time, the data for $H \geq 10$ kOe can be scaled quite well (see Fig. 11). This is evidence that, while M_f depends on temperature in lower fields, the saturated value of the ferromagnetic contribution to the sample magnetization $M_f^{(max)}$ is practically temperature independent. Indeed, as may be seen in Fig. 12, M_f , calculated according to Eq. (3), is independent of field down to $H = 10$ kOe, while the data point for

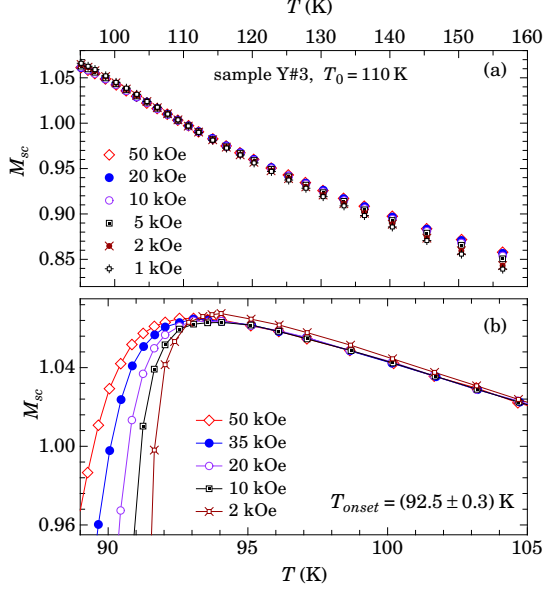


Fig. 11. M_{sc} versus T for the sample Y#2. (a) For $T > T_c$. (b) In the transition region. The solid lines are guides to the eye.

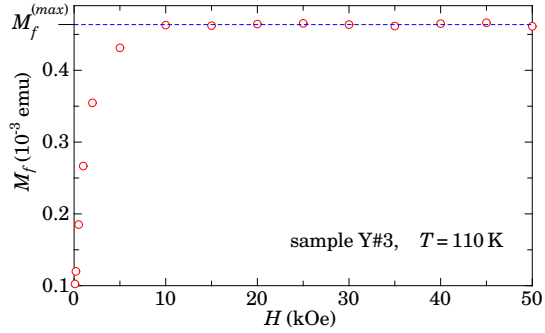


Fig. 12. $M_f = M - \chi_p H$ at $T = 110$ K as a function of H . The dashed line corresponds to $M_f^{max} = 1.64 \cdot 10^{-4}$ emu.

$H = 5$ kOe is already substantially below $M_f^{(max)}$.

3.3. Analysis of $M_{sc}(H, T)$ data below T_{onset}

Because the divergence between the $M_{sc}(T)$ curves manifests the onset of superconducting diamagnetism, the difference

$$\Delta M_{sc} = M_{sc}(H) - M_{sc}(50 \text{ kOe}) \quad (6)$$

may serve as some kind of its quantitative characteristic.

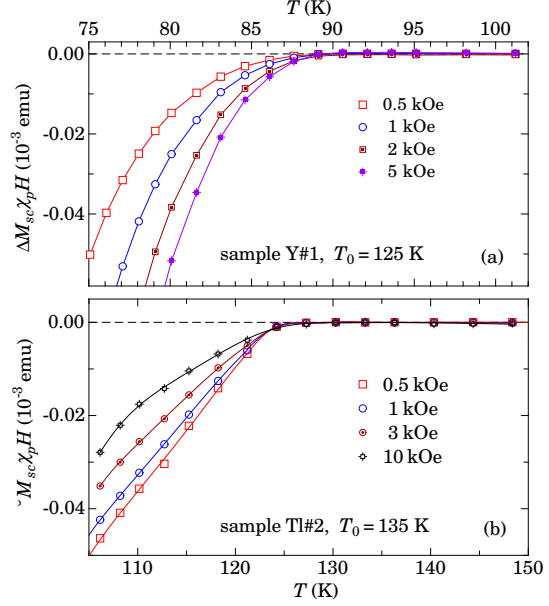


Fig. 13. $\Delta M_{sc} \chi_p H$ versus T . (a) For the sample Y#1. (b) For Tl#2. The solid lines are guides to the eye.

In order to compare ΔM_{sc} results for different values of H , it is convenient to use $\Delta M_{sc} \chi_p H$ (see Eq. (5)). Fig. 13 shows the $\Delta M_{sc} \chi_p H$ curves for the sample Y#1 and Tl#2. The values of T_{onset} resulting from this representation of the results are the same as may be determined from Figs. 10 and 11. In this case, the main source of uncertainty in T_{onset} is the distance between the neighboring data points. We also note a rather drastic difference in $\Delta M_{sc}(H) \chi_p H$ dependencies below T_{onset} for these two samples. For the sample Y#1, $\Delta M_{sc}(H) \chi_p H$ is an increasing function of H (Fig. 13(a)). Contrary to that, $\Delta M_{sc}(H) \chi_p H$ decreases with increasing H . Quite likely, this is one of manifestations of general differences between Y- and Tl-based cuprates.

4. Conclusions

The proposed approach allows to scale the normal-state magnetization $M_n(T)$ data in a way

that the $M_{sc}(T)$ curves calculated from experimental $M_n(T)$ data collected in different magnetic fields collapse onto the same master curve. Because a diamagnetic contribution to M due to superconductivity depends on magnetic field in a way, which is quite different from that for the normal-state magnetization, the onset of superconductivity leads to a rather pronounced divergence between the $M_{sc}(T)$ curves corresponding to different magnetic fields, as it may clearly be seen in Figs. 4, 8, 9, 10, 11(b) and 13. This allows for an unambiguous determination of T_{onset} corresponding to the onset of superconducting diamagnetism. Accuracy of T_{onset} is determined by an experimental scatter of $M(T)$ data and by distances between neighboring $M(T)$ data points. We remind that the proposed approach relies only on rather general properties of the normal-state magnetization and does not include any specific assumptions, which cannot be independently verified. We also note that the possibility to check the quality of scaling at temperatures well above T_{onset} serves as some consistency check. If the scaling procedure does not work satisfactory, the resulting data should not be used for important conclusions.

There are two main reasons to have quite considerable values of $(T_c - T_{onset})$. (i) Thermal fluctuations, which are expected to be especially strong in high- T_c superconductors and (ii) inclusions of small quantities of phases with higher values of T_c . Here, we mainly consider technical aspects of scaling of the normal-state magnetization data and discussion of a possible nature of the transition at $T = T_{onset}$ in different samples is beyond the scope of this paper.

Acknowledgements

This work was supported by the Swiss NCCR MaNEP II under project 4, novel materials.

References

- [1] J. Mosqueira, E. G. Miramontes, C. Torrón, J. A. Campá, I. Rasines, and F. Vidal, Phys. Rev. B **53**,

15272 (1996).

- [2] M.J. Naughton, Phys. Rev. B **61**, 1605 (2000).
- [3] A. Lascialfari, A. Rigamonti, L. Romano, P. Tedesco, A. Varlamov, and D. Embriaco, Phys. Rev. B **65**, 144523 (2002).
- [4] I. M. Sutjahja, A. A. Nugroho, M.OTjia, A. A. Menovsky, and J. J. M. Franse, Phys. Rev. B **65**, 214528 (2002).
- [5] A. Lascialfari, A. Rigamonti, L. Romano, A. A. Varlamov, and I. Zucca, Phys. Rev. B **68**, 100505 (2003).
- [6] Y. Wang, Lu.Li, M. J. Naughton, G. D. Gu, S. Uchida, and N. P. Ong, Phys. Rev. Lett. **95**, 247002 (2005).
- [7] J. Mosqueira, L. Cabo, and F. Vidal, Phys. Rev. B **76**, 064521 (2007).
- [8] S. Salem-Sugui, Jr., J. Mosqueira, and A. D. Alvarengal, Phys. Rev. B **80**, 094520 (2009).
- [9] L. Li, Y. Wang, S. Komiya, S. Ono, Y. Ando, G. D. Gu, and N. P. Ong, Phys. Rev. B. **81**, 054510 (2010).